1. Marquart, L. C., *Eine Chemisch Physiol. Abhandlung.*, Bonn, 1835.
2. Pierpoint, W. S., in *Plant Flavonoids in Biology and Medicine* (eds. Cody, V., Middleton, E. and Harborne, J. B.), Alan Liss, New York, 1986, pp. 125–140.
3. Horowitz, R. M. and Gentili, B., *J. Agric. Food Chem.*, 1969, **17**, 696–700.
4. Huang, H. T., *J. Agric. Food Chem.*, 1955, **3**, 141–146; 4a. Peng, C. Y. and Markakis, P., *Nature*, 1963, **199**, 597–598.
5. Blom, H., *Food Chem.*, 1983, **12**(3), 197–204.
6. Wesche-Ebeling, P. and Montgomery, M. W., *J. Food Sci.*, 1990, **55**(3), 731–734, 745.
7. Meschter, E. E., *J. Agric. Food Chem.*, 1953, **1**, 574.
8. Markakis, P., Livingstone, G. C. and Fellers, C. R., *Food Res.*, 1957, **22**, 117.
9. Adams, J. B. and Ongley, M. H., *Campden Food Process Assoc. Technol. Bull.*, 1972, 23.
10. Adams, J. B., *Food Manuf.*, 1973, 19th Feb.
11. Tinsley, I. J. and Bockian, A. H., *Food Res.*, 1960, **25**, 161.
12. Debicki-Pospisil, J., Lovric, T., Trinajstic, N. and Sabljic, A., *J. Food Sci.*, 1983, **48**, 411–416.
13. Nadolna, I. and Kwasniewska, I., *Przem Ferment Owocowo—Warzywny*, 1987, **31**(10), 23–26.
14. Tressler, D. K. and Pederson, C. S., *Food Res.*, 1936, **1**, 87–89.
15. Palamidis, N. and Markakis, P., *J. Food Sci.*, 1975, **40**, 1047–1049.
16. Maccarone, E., Ferrigno, Vito, Longo Maria, L. and Rapisarda, P., *Ann. Chim.*, 1987, **77**(5–6), 499–508.
17. Lukton, A., Chichester, C. O. and McKinney, G., *Food Technol.*, 1956, **10**, 427–432.
18. Nebesky, E. A., Essler, W. B., McConnell, J. E. W. and Fellers, C. R., *Food Res.*, 1949, **14**, 261–274.
19. Daravingas, G. and Cain, R. F., *J. Food Sci.*, 1965, **33**, 138–142.
20. Francis, F. J. and Starr, M.S., *Food Technol.*, 1968, **22**. 1293–1295.
21. Clydesdale, F. M., Main, J. H., Francis, F. J. and Damon, R. A., *J. Food Sci.*, 1978, **43**, 1687–1697.
22. Beattie, H. G., Wheeler, K. A. and Pederson, C. S., *Food Res.*, 1947, **8**, 395.
23. Pederson, C. S., Beattie, H. G. and Stotz, E. H., *N. Y. Exp. Stat. Bull.*, 1947, **72**, 8.
24. Shrikhande, A. J. and Francis, F. J., *J. Food Sci.*, 1974, **39**, 904–906.
25. Karrer, P. and De Meuron, G., *Helv. Chim. Acta*, 1932, **15**, 507.
26. Hradzina, G. H., *Phytochemistry*, 1970, **9**, 1647.
27. Jurd, L., in *Anthocyanin Type Plant Pigments, The Chemistry of Plant Pigments*, Academic Press, New York, 1972.
28. Mikova, K., Havlikova, L. and Mocova, A., *Sb. Vys. Sk. Chem.-Technol. Praze Potraviny*, 1986, **E60**, 37–49.
29. MacKinney, G., Lukton, A. and Chichester, C. O., *Food Technol.*, 1955, **9**, 324–326.
30. Culpepper, I. W. and Caldwell, J. S., *J. Agric. Res.*, 1927, **35**, 107.
31. Salt, F. W. and Thomas, J. G. N., *J. Appl. Chem.*, 1957, **72**, 31.
32. Cichon, Z. and Kolek, Z., *Przem. Spozyw.*, 1991, **45**(10), 255–258.
33. Cichon, Z. and Kolek, Z., *Przem. Spozyw.*, 1991, **45**(8), 195–199.
34. Jurd, L., *J. Food Sci.*, 1964, **29**, 16.
35. Esslen, W. B. and Sammy, G. M., *Food Prod. Div.*, 1973, **7**(1), 80.
36. Esslen, W. B. and Sammy, G. M., *Food Prod. Div.*, 1975, **9**(1), 37.
37. Garoglio, P. G., in *La Nuvoa Enologia*, 3rd ed, Inst Ind Firenze, Italy, 1965.
38. Metevier, R. P., Francis, F. J. and Clydesdale, F. M., *J. Food Sci.*, 1980, **45**, 1099–1100.
39. Shewfelt, R. L. and Ahmed, E. M., *J. Food Sci.*, 1978, **43**, 435–438.
40. Lowry, J. B. and Chen, L., *Econ. Bot.*, 1974, **28**, 61–62.
41. Anonymous, *Food Eng.*, 1978, **50**, No 12ef-14.
42. Saito, N., Abe, K., Honda, T., Timberlake, C. F. and Bridle, P., *Phytochemistry*, 1985a, **24**, 1583.
43. Timberlake, C. F. and Bridle, P., in *Developments in Food Colours* (ed. Wallford, J.), Appl. Sci. Publ., London, 1980, pp. 115–149.
44. Timberlake, C. F. and Henry, B. S., *Endeavour* (*News Ser*)., 1986, **10**, 31.
45. Asen, S., Stewart, R. N. and Norris, K. N., U. S. Patent, 4 172 902, 1979.
46. Kotake, K., JP 62 19068 (87 19068), 1987.
47. JP 62 115 069 (87 115 069), 1987.
48. Hasegawa, T., JP 58 65 761 (83 65 761), 1983.
49. Maccarone, E., Maccarone, A. and Rapisarda, P., *Int. J. Food. Sci. Technol.*, 1987, **22**(2), 159–162.
50. Harborne, J. B., Mayer, A. M. and Bar-Nun, N., *Z. Naturforsch.*, 1983, **38c**, 1055.
51. Oohashi, Y., Mizukami, H., Tomita, K., Hiasoka, N. and Fujimoto, K., JP 01 30 594 (89 30 594), 1989.
52. Saquet-Barel, H. and Crouzet, J., LWT—ed., *Prog. Food Eng.*, 1983, 573–580.

Received 30 October 1992; accepted 16 November 1992.

High latitude–low latitude ionosphere coupling

V. V. Somayajulu and Ligi Cherian

Space Physics Laboratory, Vikram Sarabhai Space Centre, Trivandrum 695 022, India

This article examines the strong electrodynamic coupling between the high, middle and low latitude ionospheres using interplanetary magnetic field data together with the electric fields obtained from the Doppler frequency variations of the coherent VHF backscatter signals at Trivandrum, plasma drift measurements in the F region from the incoherent scatter radar, ground-based magnetograms from high, middle and low latitudes including the equatorial region. The virtual height variations obtained from ionograms during the post-midnight sector are used to show that the global convection models reproduce a number of characteristics of low latitude and equatorial electric fields associated with changes in the polar cap potential drop. In addition, we highlight several areas of substantial disagreement between the electric field data and the theoretical results.

DURING the last two decades, significant progress has been made in elucidating the magnetosphere-ionosphere-thermosphere coupling processes at high latitudes[1]. One of the important features of the dynamic

magnetosphere-ionosphere system is the strong electrodynamic coupling between the ionospheric and magnetospheric plasma along the highly conducting high latitude magnetic field lines. For example, electric fields generated due to solar wind-magnetosphere dynamo are mapped down along the geomagnetic field lines into the polar cap where the electric field is aligned roughly from dawn to dusk and this electric field induces a large scale convective motion in the high latitude ionosphere[2]. The strong solar wind-magnetosphere coupling also produces a system of plasma convection away from the sun in the outer magnetosphere and in the magnetically connected high latitude ionosphere, whereas the plasma in the inner magnetosphere which is connected magnetically to the ionosphere at low latitudes flows sunward to complete the circulation pattern[3]. The dawn–dusk electric field is thought to be partly shielded from the inner magnetosphere and hence from the middle and low latitude regions by the geomagnetic ring current[4,5]. However, on certain occasions, a portion of the electric field that penetrates to middle and low latitudes has been detected by the effect it produces on the plasma drifts[6–10] (Ref 7 gives an excellent review on plasma drifts). Now, it is well recognized that the response of the middle and low latitude ionosphere including equatorial dynamo region of the ionosphere (90–140 km) to the polar-auroral region dynamo processes can manifest itself in two ways[7,11]. One is the impulsive penetration of the electric fields and currents from the magnetosphere and high latitude ionosphere to middle and low latitudes during magnetic storms and substorms[12–15]. The second mechanism is due to the dynamo action of the storm time thermosphere winds produced by the Joule heating of the auroral electrojets. These winds alter the global circulation pattern and generate disturbance dynamo electric fields at middle and low latitudes[15] which are westward during daytime and eastward at night-time and they act in opposition to the normal quiet day electric field variations.

The electrodynamical coupling between the high and low latitude ionosphere has been studied from the close correlation between the large fluctuations in the intensities of the equatorial and auroral electrojets based on the geomagnetic data obtained from the flux gate magnetometers located at remote places on the earth's surface[17–22]. Further, the electric field observations using incoherent and coherent backscatter radars during the last decade have made remarkable progress, not only in terms of elucidation of the large scale convection pattern over the polar region but also provided extensive and valuable information on the electric fields in the equatorial, middle and auroral regions under a wide variety of geomagnetic disturbance conditions[3,6,7,12–15,23–28]. However, the ground-based observations from magnetometers, incoherent radars, VHF backscatter radars and Ionosondes have to be supplemented with satellite observations of IMF, solar wind velocity (V) and density (n) as well as the magnetic indices derived from ground-based observations such as auroral electrojet indices (AU, AL, AE and AO) and the ring current index (D_{st}). Based on these data sets, good progress has also been made in the study of three-dimensional current systems during magnetospheric substorms, in particular, the relationship between field aligned currents, ionospheric currents, the convective electric field, discrete and diffuse aurora and auroral electron spectra[29]. Such a variety of observations have begun to converge in providing a self-consistent model of solar wind-magnetosphere-high latitude dynamo region-low latitude dynamo region coupling.

The penetration of high latitude electric fields into the low latitude ionosphere has also been studied in detail during the last two decades using numerical simulations of ionospheric electric fields and currents in relation to field aligned currents[30–41]. These have shown that simulation studies are a powerful tool in unveiling physical processes occurring in the ionosphere-magnetosphere system during substorms. In this paper, we present a brief outline of the most important earlier results and then discuss in greater detail the recent experimental and theoretical studies as well as some of the critical problems which will hopefully be clarified in the next few years.

Distribution of equatorial zonal electric fields

Effect of north-south component (B_z) of interplanetary magnetic field (IMF)

Several attempts have been made to assess the direct correlation between the time variation of IMF B_z component as measured by satellites and the radar-measured vertical drift velocities in the F-region or the ground level magnetometer measured changes of electric fields or currents in the middle- and low-latitude ionosphere[26,42–47]. All these studies indicate good correlation in some cases and absence of correlated changes between IMF and equatorial ionospheric electric fields. This is probably due to the fact that the effect of IMF B_z on equatorial ionospheric electric fields is not likely to be direct or simple because a chain of physical processes are involved both in the outer and inner magnetospheres due to solar wind–magnetosphere interactions. Figure 1 shows the time variation (full line) of the mean Doppler frequency (f_D) of the 2.7 m scale size irregularities measured with a coherent VHF backscatter radar operating at Trivandrum (Geog. Lat. 8.2 N, Geog. Long. −77° E, Dip −0.5° S). The geometry of the radar antenna[13] is such that the negative (positive) f_D variations

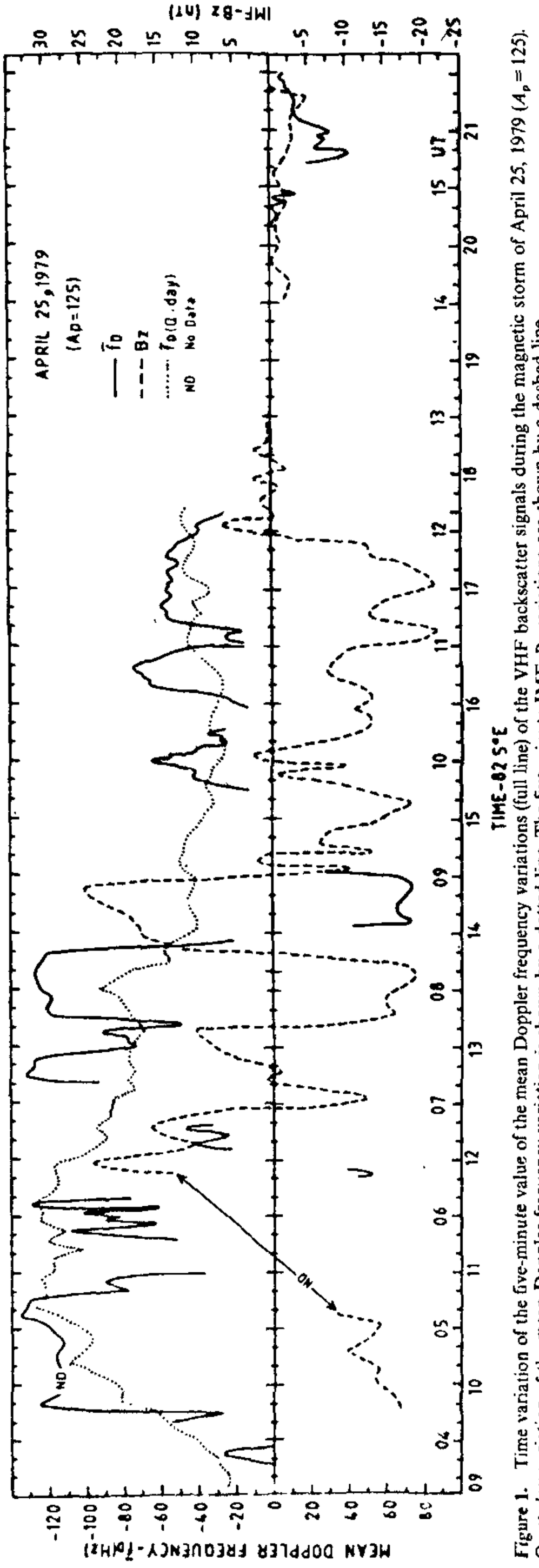

Figure 1. Time variation of the five-minute value of the mean Doppler frequency variations (full line) of the VHF backscatter signals during the magnetic storm of April 25, 1979 ($A_p = 125$). Quet day variation of the mean Doppler frequency variation is shown by a dotted line. The five-minute IMF B_z variations are shown by a dashed line.

correspond to westward (eastward) movement of the irregularities in the presence of eastward (westward) electric field. The f_D variations of the VHF radar signals backscattered from the electrojet plasma irregularities of type II are proportional to the east-west electric field causing the drift motion of the irregularities and as such the f_D variations represent the driving east-west electric fields in the equatorial electrojet. Also shown as dashed curve in Figure 1 are 5-minute values of the temporal variation of the IMF north-south(B_z) component. The dotted curve shows the quiet day (March 21, 1979, $A_p = 5$) f_D variations. The large rapid fluctuations of f_D on magnetic storm day in comparison to quiet day show that the electrojet behaviour on storm days is controlled by the electric fields originating in the magnetosphere-ionosphere interactions. An interesting aspect to be noted is the time delay of about 15–20 minutes between the IMF-B_z turning southward from northward or vice-versa and the appearance of radar signals with strong eastward field or westward electric field (as shown by negative and positive f_D variations). The northward turning of IMF at 1240 IST (Indian Standard Time, IST, 82.5° E) is associated with a decrease in f_D and finally when the IMF turns northward at 1345 it is followed by a westward field from 1400–1430 IST. At later times (between 1520 and 1740 IST) whenever the IMF B_z southward component decreases, a corresponding decrease in the eastward field is observed. Further, on certain occasions, the absence of radar signals when the IMF B_z is northward shows the presence of a westward electric field superimposed over the normal eastward electric field expected at those times (quite day values are shown by a dotted curve). The radar observations thus show unambiguously that the electric fields in the equatorial electrojet region do get reversed quiet often when the IMF B_z turns northward. Another notable feature is the enhanced eastward electric field (negative f_D) from 1500–1740 IST when the IMF B_z component is essentially southward. Here again, when the IMF B_z southward component decreases or turns northward, radar signals are absent thereby showing clearly that the equatorial electrojet electric field responds very sensitively to the IMF fluctuations. For completeness, we show in Figure 2 an example of large daytime vertical drift variations observed with Jicamarca radar[6] during a period of large changes in the IMF (northward turning at 1100 LT is followed by a downward drift and southward turning at 1300 LT is followed by an upward drift) and the auroral current system[6]. However, Sastry[14] showed (Figure 3) that high variance of IMF just around the times of northward turning of B_z facilitates a prompt and effective decrease of magnetospheric convection related electric field. As a consequence, the shielding charges in the inner magnetosphere produce a dusk-to-dawn electric field

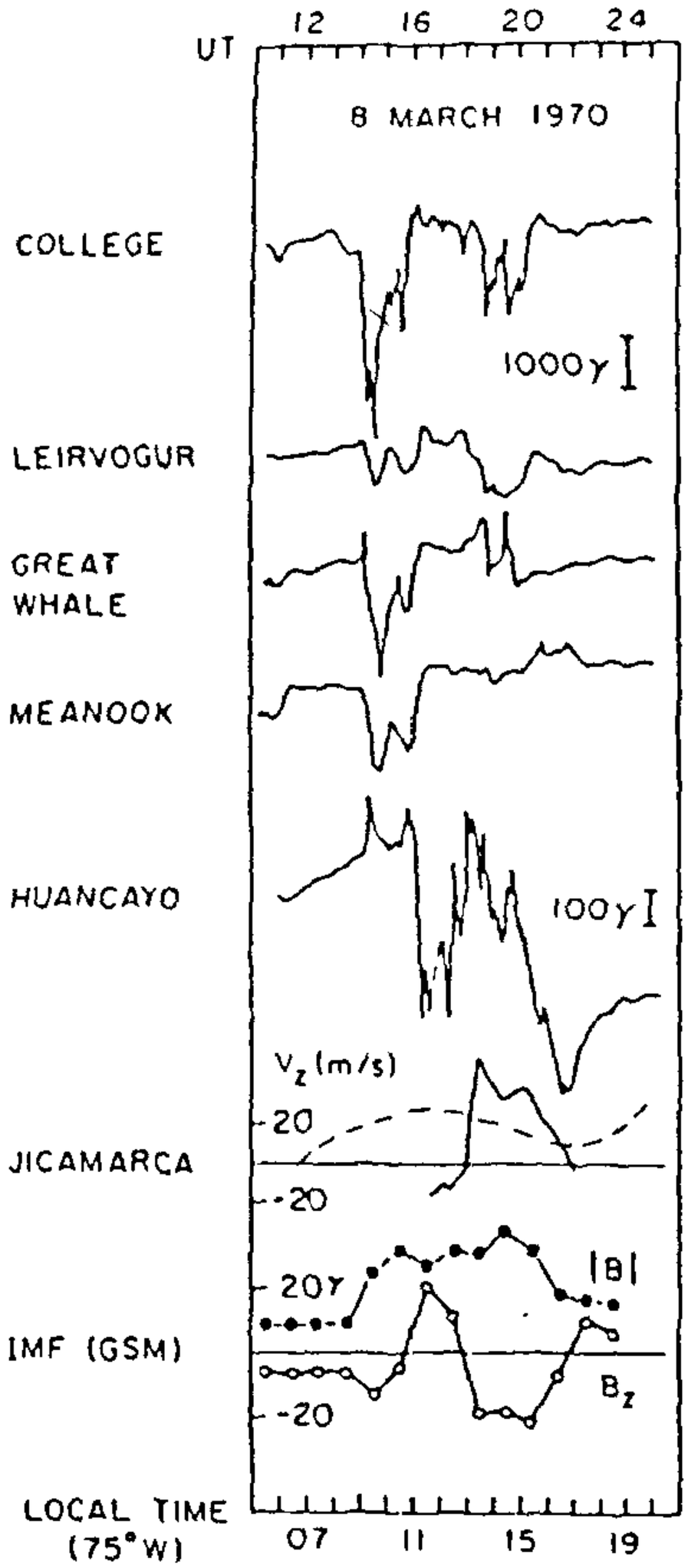

Figure 2. Daytime vertical drift velocity (east-west electric field variations in the *F* region measured with Jicamarca radar during the magnetic storm of March 8, 1970. The associated high latitude magnetograms and IMF B_z variations are also shown (after Fejer *et al.*[26]). The dashed curve on the V_z plot represents the quiet-time pattern of V_z.

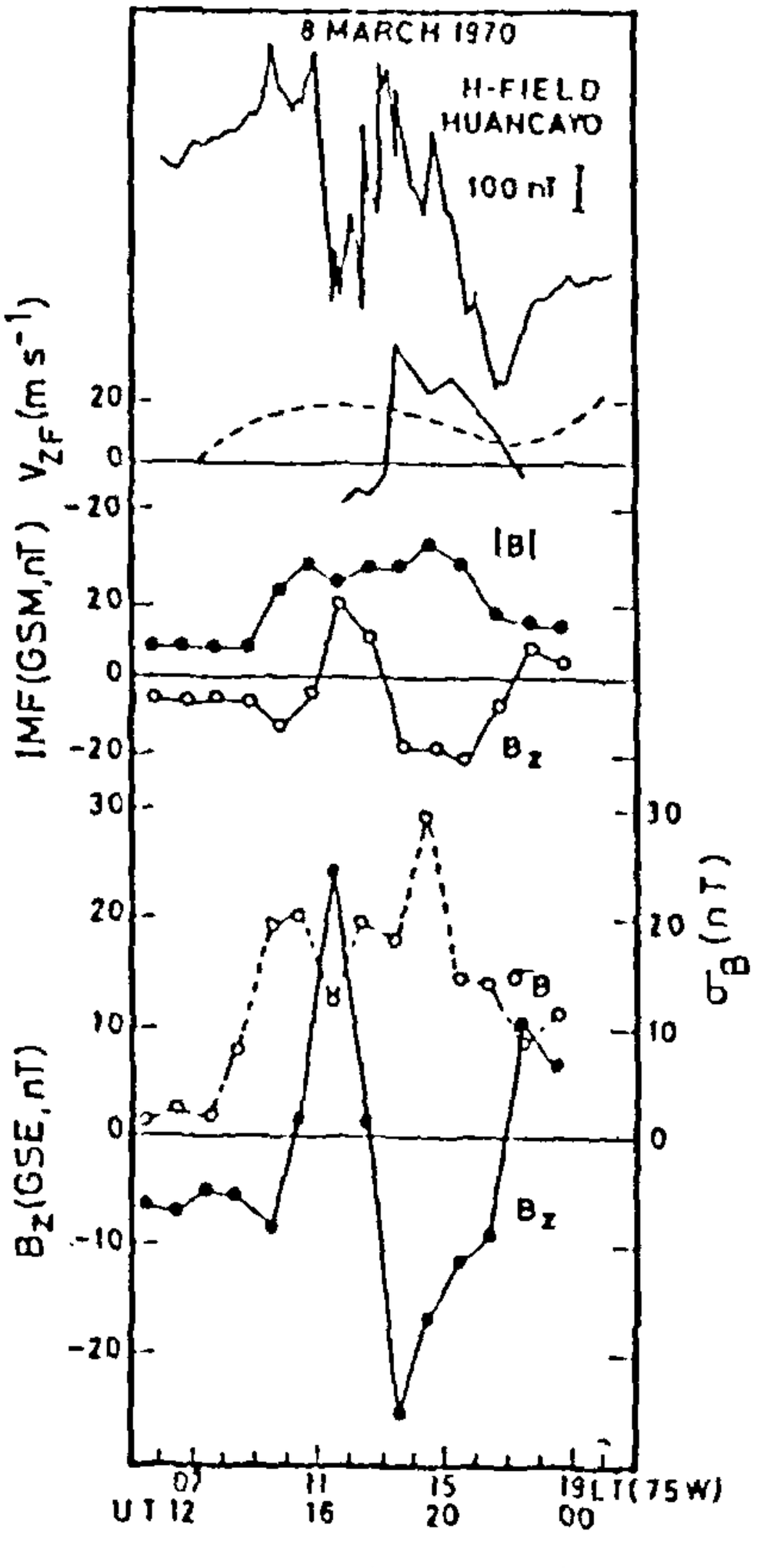

Figure 3. Same as Figure 2 without high latitude magnetograms. The bottom panel shows the B_z (in GSE co-ordinates) and variance of *IMF* (σ_E) *during March 8, 1970* (Sastry[14]).

which then penetrates into the low latitude ionosphere.

Measurement of east-west drift velocities of the equatorial electrojet irregularities during night-time with a VHF backscatter radar is very difficult because of the low electron density and hence low conductivity. However, equatorial *F* region vertical drift velocities using incoherent scatter radar and the rate of change of virtual height variations measured from the ionograms during night-time can be effectively used to study the night-time high latitude-low latitude ionosphere coupling. The rate of change of virtual height variations of the bottom side of equatorial *F* region represents the vertical electrodynamic drift velocity (due to eastward electric fields) after correcting for the apparent vertical drift due to chemical loss. A drift velocity of 25 m/s corresponds to 1 m V/m electric field at *F* region heights at Trivandrum. Figure 4 shows the sudden increase in vertical drift velocity on 23–24 November 1986 where the IMF B_z (shown as a full line) has turned northward at about 2300 UT (shown by a vertical

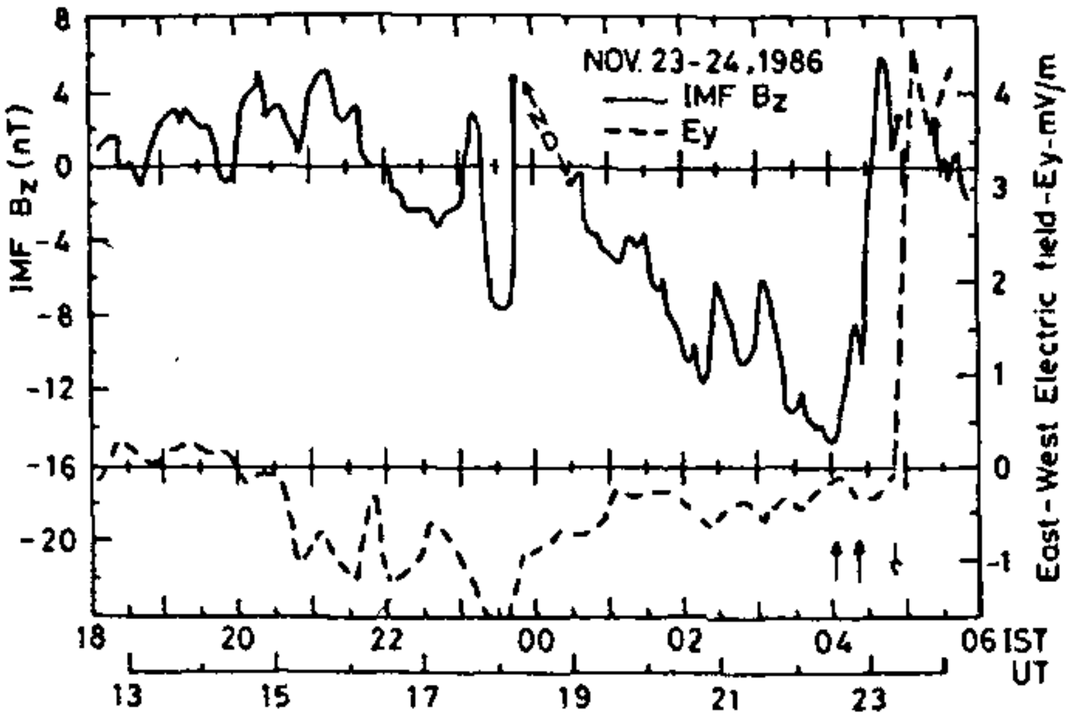

Figure 4. Time variation of the east-west electric field obtained from the rate of change of virtual height variation deduced from quarter hourly ionograms during November 23–24, 1986. The IMF B_z values are shown by a full line (adapted from Somayajulu *et al.*[47]).

dotted line). Associated with this northward turning of IMF B_z, the magnetic field (shown Figure 5) started to increase in the positive direction at auroral and polar stations indicating an enhancement of the eastward polar electrojet current[47].

From the above, it is clear that zonal electric field changes related to southward B_z are eastward on the dayside and westward in the night side whereas the large northward B_z turnings are associated with westward fields during daytime and eastward during night-time[14,47]. Furthermore, some of these electric field changes are not driven directly by the IMF changes but also are the result of changes in the magnetospheric convection and substorm phenomena[7,13].

Nature of substorm related transient disturbances

From earlier results, it is clear that the amplitude and frequency of the transient electric field disturbances at low latitudes due to sudden IMF changes and substorm activity are thus quite asymmetric. This is understandable because the auroral-polar electrojets may be produced by multiple current systems such as solar-driven 'convection electrojet' and also in part by the sub-storm 'expansion phase electrojet' whose importance may vary spatially around the electrojet region and temporally during the event. More specifically, the electric fields associated with the plasma convection drives a two-cell current system in the polar ionosphere known as DP2 current system[21,48], which is interpreted as the manifestation of a process directly driven by the solar wind, whereas, the accumulation of magnetic flux in the tail lobe (loading) and subsequent release of the stored energy from the tail lobe (unloading) gives rise to a westward electrojet.

Figure 6*a* represents the variations in the zonal

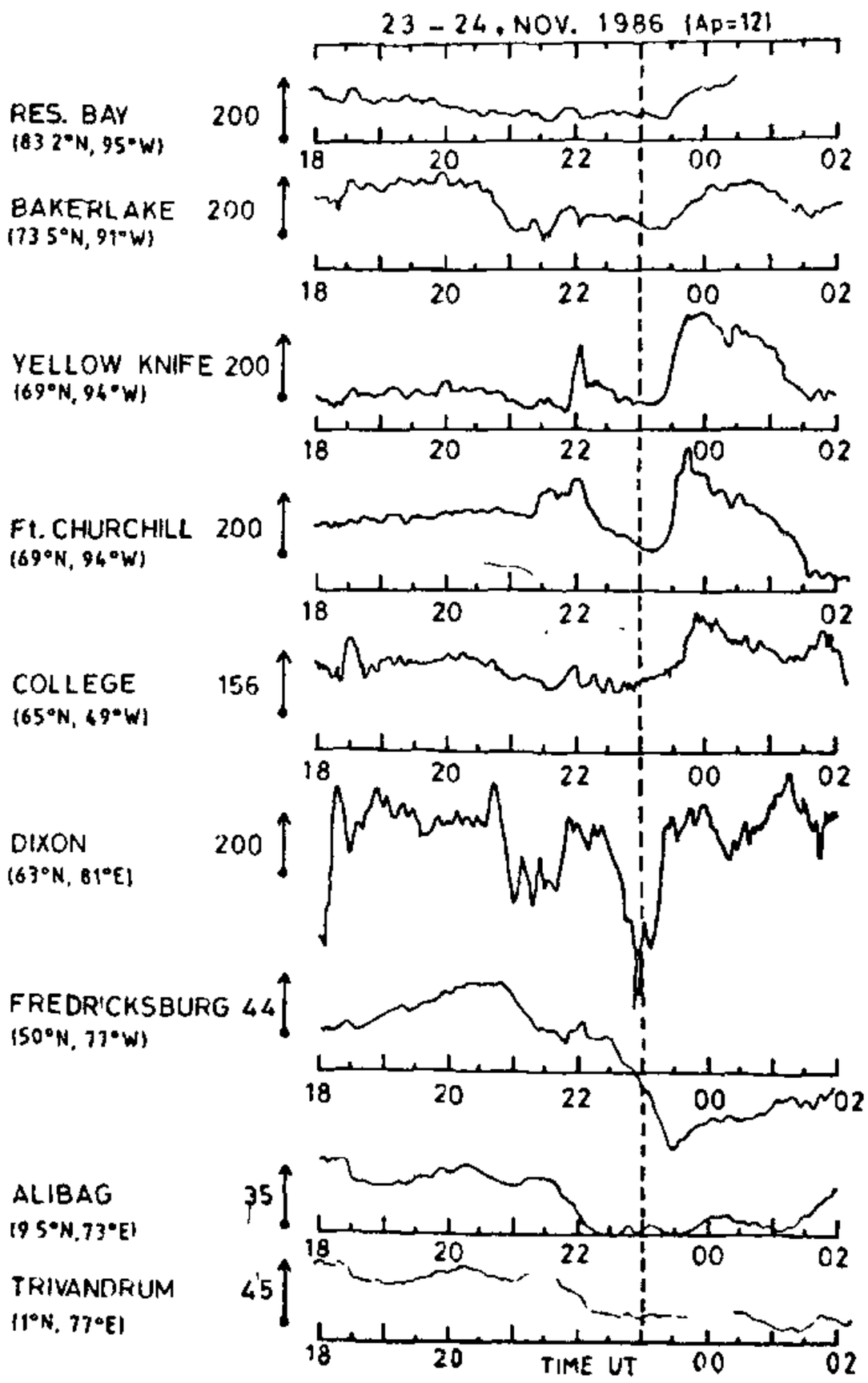

Figure 5. Time variation of the horizontal component of the earth's magnetic field at high, middle and low latitude stations on 23–24, November 1986 (adapted from Somayajulu *et al.*[47]). The geomagnetic latitude and geographic longitude of the stations are shown. The vertical arrows for each station show the scale values of the magnetic field. The dashed line at 2300 UT indicates the time at which IMF B_z has turned northward.

electric field at equatorial electrojet altitudes during the March 22, 1979 substorm event identified by the co-ordinated Data Analysis Workshop (CDAW6). The IMF B_z turning southward at 1008 UT (Figure 6*c*) is followed by a growth phase from 1020–1050 UT. The onset of the expansion phase is identified to be at 1054 UT. Further, the southward turning of IMF at 1008 is followed by a sudden increase in the polar cap equivalent current at 1020 UT indicating enhanced convection driven by solar wind[49]. The enhanced polar cap current system is associated with a rapid increase in the eastward electric field at equator by a factor of 2. However, the signal strength (Figure 6*b*) of the irregularities increases by a factor of 5 clearly showing that the electric field has probably changed by that

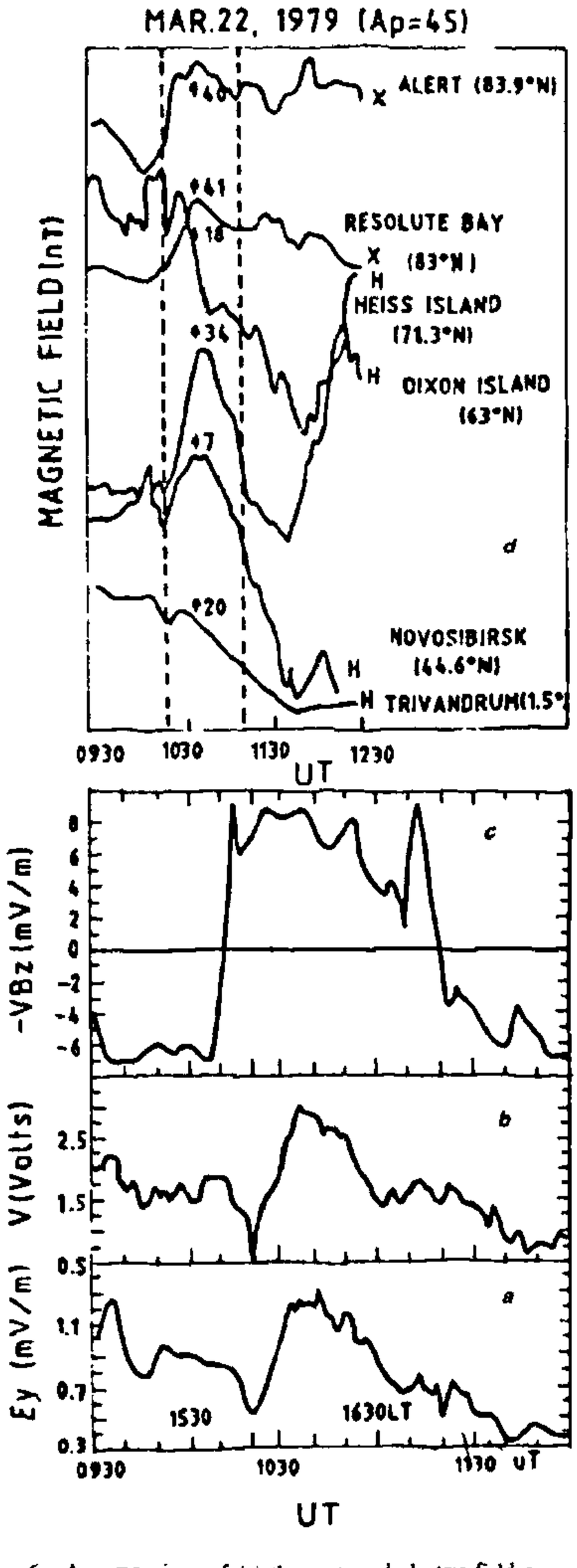

Figure 6. A comparison of (*a*) the eastward electric field computed from the mean Doppler frequency variations of the VHF backscatter radar signals, (*b*) signal strength of the VHF backscatter radar signals and (*c*) the solar wind coupling function ($-V_{sw}\,B_z$) during the growth phase of the magnetic storm (0930–1130 UT) on March 22, 1979 (Somayajulu *et al.*[47]) and (*d*) variations of the horizontal component of the earth's magnetic field at selected polar, auroral and midlatitude stations during the growth of phase of the magnetic storm on March 22, 1979 (Somayajulu *et al.*[47]).

factor[13]. Thus the rapid increase in the eastward electric field is a clear response to the increase of convection electric field changes arising from the solar wind energy coupling to the magnetosphere. The high latitude magnetograms (Figure 6 *d*) show an increase in the horizontal component$^{(H)}$ of the earth's magnetic field at 1020 UT indicating an enhancement in the eastward auroral electrojet in all the time sectors (for details see Mcpherron and Manka[49]). The auroral zone station of Dixon and the mid-latitude station of Novosibirsk in the late afternoon sector also show a positive bay in H at 1020 UT. However, an increase in the H component occurs at Trivandrum at 1020 UT, but the later part of the positive bay is obscured by the main phase decrease resulting from the ring current development (for details see Somayajulu *et al.*[13]). Using the ground magnetometer inversion scheme Clauer and Kamide[50] computed the equivalent current patterns as well as the real ionospheric and field-aligned current distributions during the growth phase (1020–1050 UT) of the above substorm. The growth phase of the substorm is characterized by the gradual enhancement of a DP2 equivalent current system following the southward turning of the IMF (Figure 7). There are two electrojets centered at dusk and dawn and the intensities of these electrojets are nearly the same. The pattern of the calculated field aligned currents is somewhat irregular, but one can still identify the currents of regions 1 and 2 and the downward current in the dayside cusp.

Effect of polar cusp variations

Various satellite measurements have confirmed the existence of a pair of neutral points called the 'polar cusp' of 'dayside cleft' at about 76° geomagnetic latitude in both the hemispheres. It is also known that the solar wind particles entering through these regions in the dayside magnetosphere populate the high latitude ionosphere. It is observed that, in general, the polar cusp shifts equatorward during the southward direction of the IMF and moves poleward in the presence of northward IMF. The large equatorward movement of the polar cusp region has been explained by Meng[51] in terms of the interaction between the north-south component of the IMF and geomagnetic field in the magnetosphere. In the following, we study the effect of polar cusp position on the equatorial electrojet electric fields. Figure 8 shows the time variation of the horizontal component of the earth's magnetic field at Trivandrum and the IMF B_z component (dotted line) during the magnetic storm of September 18, 1979. Also shown are the D_{st} index (filled triangles) and the variation of the polar cusp position and its width in northern hemisphere (vertical line) and in the southern hemisphere (dashed vertical line). The time variation of cusp position is obtained from observations of the very soft but intense electron precipitation detected[51] by the low energy detectors

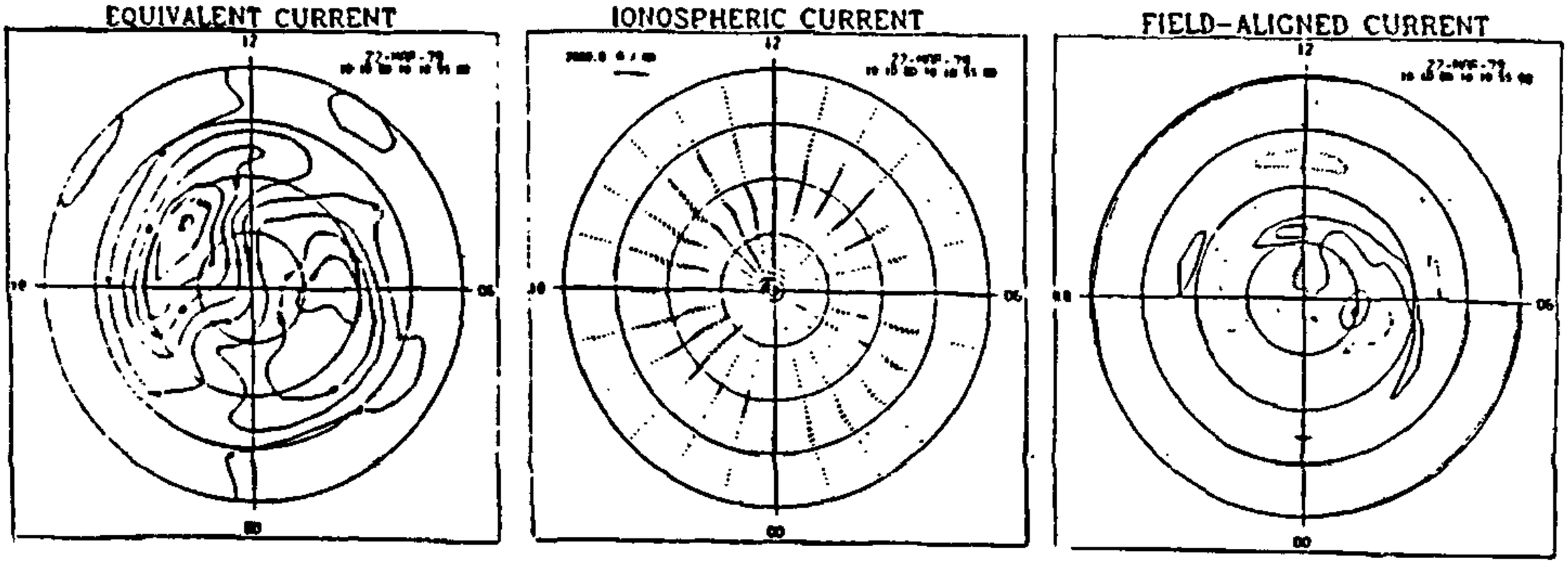

Figure 7. Equivalent current, ionospheric and field-aligned current distributions which develop during the interval 1010 to 1050 UT on 22 March 1979 corresponding transient electric field disturbance observed at Trivandrum (shown in Figure 6). Equivalent current contours are drawn at 80,000 A intervals. Relative maxima are indicated by plus and minus signs. Contour levels for the distribution of field-aligned currents are plotted at 0.5×10^{-6} A/m^2. Downward current is indicated by solid lines and upward current is indicated by dashed lines. Latitude circles are drawn at 10° intervals. The outer boundary of each plot is 50° latitude (Clauer and Kamide[50]).

onboard the DMSP satellites F_2 and F_4. The bottom panel shows the Doppler frequency variations of backscattered signals observed at Trivandrum during the magnetic storm. It is at once clear that the long-term trend (9–10 hours) in the variation of the eastward electric field in the equatorial electrojet (as represented by f_D variations in Figure 8) reveals that the magnetospheric and high latitude electrodynamic changes which are concurrent in time with the changes in the polar cusp latitude during a geomagnetic storm give rise to a large westward electric field in the equatorial electrojet region. We believe that the observed relationship between the changes in the polar cusp regions and the electric fields in the equatorial electrojet region can be explained in terms of the large scale electric field changes in the polar-auroral dynamo region due to fluctuations in the IMF north-south component or the direct penetration of the magnetospheric electric fields to low latitudes. This is logical because the movement of the cusp latitude is only one of the manifestations of several large scale electrodynamical processes that take place in the inner magnetosphere during geomagnetic storms and substorms.

Discussions and conclusions

During quiet geomagnetic conditions, electric fields of neutral wind dynamo origin predominate at middle and low latitudes. However, during disturbed geomagnetic conditions, extensive and compelling evidence shows that a close electrodynamic coupling exists between the high latitude and the low latitude ionospheres. The response of the low latitude electric fields to changes in the high latitude current systems can be divided into two main categories. The electric field disturbances of first category which propagate almost instantly from high latitudes to middle and low latitudes are due to the sudden perturbations in the magnetospheric potential across the polar cap that lasts for one to two hours. The second category of electric field perturbations is due to the disturbance dynamo effects that propagate equatorward with latitude-dependent time delays of the order of 2–10 hours. It is usually very difficult to separate the direct penetration and disturbance dynamo components from the observed electric field variations.

The observed zonal electric field perturbations are usually westward during the day and eastward at night, and are often associated with large and sudden decreases in high latitude convection driven by rapid changes of northward IMF[26,45]. The typical daytime westward perturbations have values of 0.3 mV/m while the night-time eastward electric fields have large amplitudes of about 1.5–3 mV/m especially in the early morning (02–05 LT) sector and smallest amplitudes between dusk and midnight[6,7].

The physical mechanisms which govern the strength and duration of electric field perturbations at middle and low latitudes due to IMF B_z variations is theoretically uncertain at the present time as it most likely involves subtle points of magnetospheric physics as well as details of magnetosphere-ionosphere-thermosphere coupling[7]. Accordingly, the present-day quantitative models are somewhat uncertain on these points. In the following discussion, we present a brief outline of the various mechanisms proposed to explain the prompt penetration of magnetospherically generated electric fields to the middle and low latitudes ionosphere.

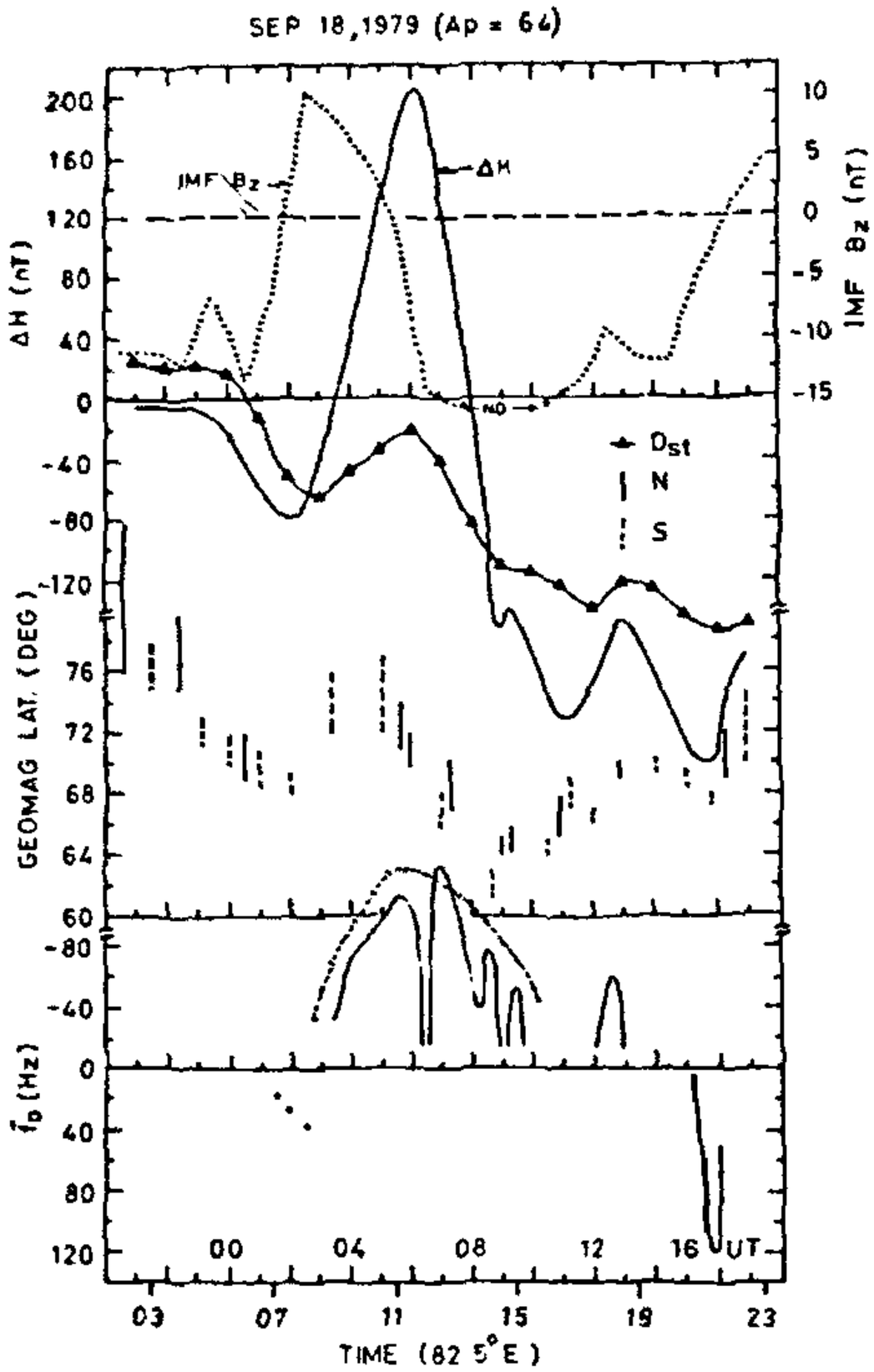

Figure 8. Time variations of the mean Doppler frequency (f_D) of the backscatter signals from the 2.7 m scale size irregularities in the equatorial electrojet on September 18, 1979 ($A_p = 64$). The curve (...) represents the quiet-day variations of the f_D. The middle panel shows the latitude and width of the polar cusp position in the northern hemisphere (vertical full line) and southern hemisphere (dashed vertical line). The top panel shows the variation of the horizontal component of the earth's magnetic field at Trivandrum (full line) and the IMF B_z variation (dotted line). Filled triangles show the variation of ring current index (D_{st}).

Kelley *et al.*[45] proposed that the observed transient electric fields associated with northward IMF turnings cause a temporary imbalance between convection-related charge density and the charge on the inner edge of the magnetosphere due to the sudden decrease of the convection electric field. This mechanism generates a dusk-dawn perturbation electric field during a period (several minutes to one hour) of the order of the time constant for the decay of the shielding charges. This transient electric field perturbation due to the 'over shielding' of the inner magnetosphere is westward on the dayside and eastward on nightside in agreement with the observations. A similar process occurs during periods of sudden increase in convection when the night-time shielding layer moves equatorward and the 'under shielding' of the inner magnetosphere generates a dawn–dusk transient electric field.

Numerical simulation studies to understand the penetration of high latitude electric fields into the middle and low latitude ionosphere have proceeded in two different lines. In one approach model calculations using empirical high latitude field aligned currents explain the general form of the middle and low latitude perturbation potential and of the corresponding electric fields[28,31,36–41]. However, since magnetospheric processes are not included in these models, the calculations are not self-consistent and cannot determine the time evolution of perturbation electric fields. Recently, more detailed semi-analytical models based on the convection approach of Vasyliunas (presented by Senior and Blanc[35] and Spiro *et al.*[33]) provide detailed information on the transient electric field response at middle and low latitudes to changes in high latitude convection[28,33]. The models predict correctly that a decrease in convection associated with a rapid northward turning of IMF generates a westward electric field perturbation on the dayside and eastward at night. In addition, the overshielding mechanism does not generate electric fields with large enough amplitudes. Recently A. D. Richmond[28] suggested that thermospheric 'fossil winds' might play a significant role on the generation of perturbation electric fields following sudden geomagnetic quietening (Figure 9 illustrates the mechanism).

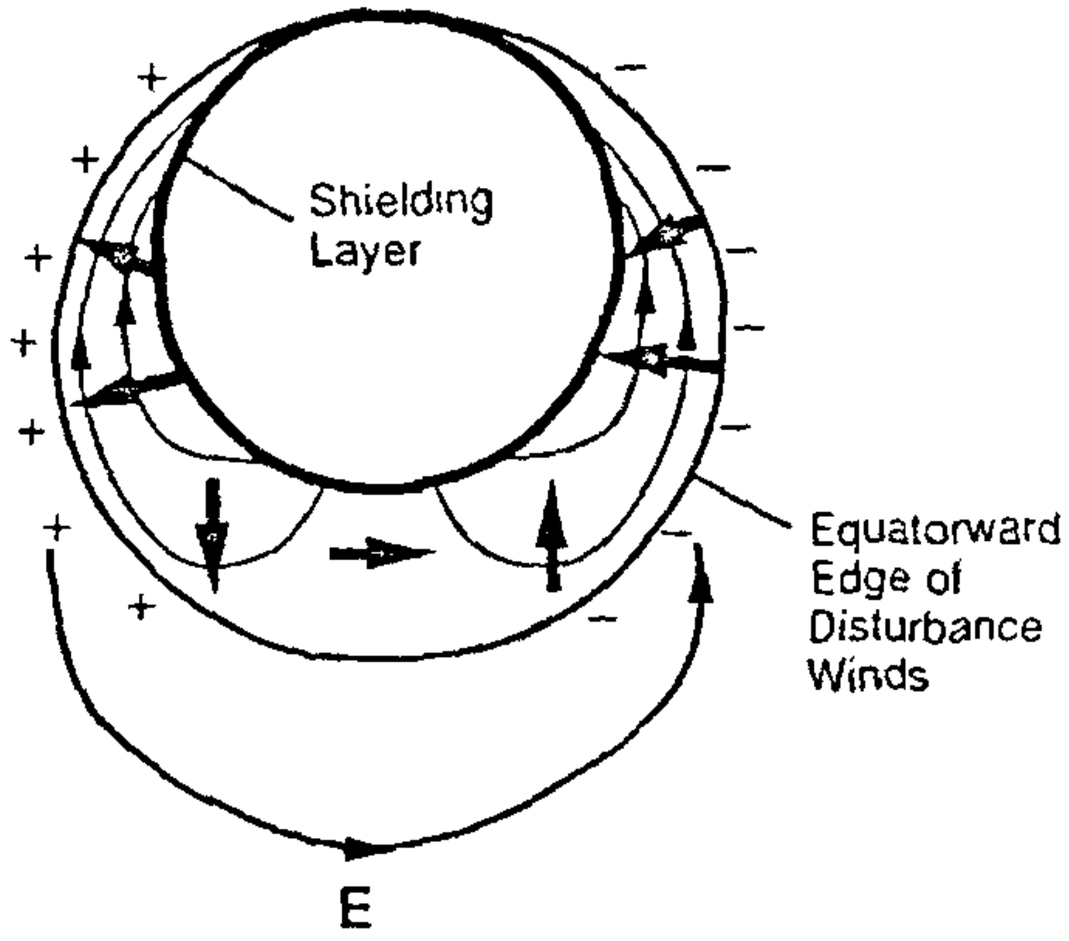

Figure 9. A sketch of the 'fossile wind' mechanism for the generation of middle- and low-latitude perturbation electric fields following a sudden decrease in the polar cap potential. The two circles represent the locations of the equatorward edge of the disturbance winds, and of the shielding layer which has moved poleward. The thin contour lines correspond to the neutral wind flow pattern and the arrows represent the pedersen currents driven by the disturbance winds. The positive charges pile up on the dusk and the negative charges on the dawn side of the equatorward edge of the winds, generating a dusk-to-dawn electric field at middle- and low-latitudes (Fejer *et al.*).

Spiro *et al.*[33] and Fejer *et al.*[28] observed that the fossil wind effects increase the time constant of the decay of the electric fields but do not change the daily patterns.

Outstanding problems and conclusions

The understanding of the variation of electric fields during magnetically disturbed periods is considerably less clear because of the difficulties associated with the high resolution measurements using incoherent radars and backscatter radars. Further, the high degree of complexity of the high latitude processes which control the electric field penetration to lower latitudes are poorly understood. Therefore, it is suggested that high time resolution measurements during storms and substorms over a range of longitudes and latitudes using incoherent and coherent backscatter radars, chain of ionosondes and magnetometers are necessary for a better understanding of the high latitude–low latitude ionosphere coupling.

1. Schunk, R. W., Proceedings of the XXVII COSPAR Plenary Meeting, 1988, pp. 52–110.
2. Rostoker, G., in *The Solar Wind and the Earth*, (eds. Akasofu, S. I. and Kamide, Y.), Terra Scientific Pub Co., Tokyo, 1987, pp. 163–181.
3. Kelley, M. C. and Heelis, R. A., *The Earth's Ionosphere-Plasma Physics and Electrodynamics*, Academic Press, London, 1989, pp. 261–301.
4. Wolf, R. A., *Space Sci. Rev.*, 1975, **17**, 537–560.
5. Mank, B. H. and Zanetti L. J., *Rev. Geophys.*, 1987, **25**, 541–554.
6. Fejer, B. G., in *Solar Wind-Magnetosphere Coupling* (eds. Kamide, Y. and Slavin, J. A.), Terra Scientific Pub Co., Tokyo, 1986, pp. 519–545.
7. Fejer, B. G., *J. Atmos. Terr. Phys.*, 1991, **53**, 677–693.
8. Rastogi, R. G., *Geomagnetism*, 1989, **3**, 462–525.
9. Ganguly, S., Behnke R. and Emery B. A., *J. Geophys. Res.*, 1987, **92**, 1199–1204.
10. Reddy, C. A., *Pure Appl. Geophys.*, 1989, **131**, 485–508.
11. Kamide, Y., *J. Geomag. Geoelectr.*, 1988, **40**, 131–155.
12. Somayajulu, V. V., Reddy C. A. and Viswanathan K. S., *Geophys. Res. Lett.*, 1985, **12**, 473–476.
13. Somayajulu, V. V., Reddy C. A. and Viswanathan K. S., *Geophys. Res. Lett.*, 1987, **14**, 876–879.
14. Sastry, J. H., *Planet. Space Sci.*, 1988, **36**, 785–790.
15. Sastry, J. H., *Ann. Geophys.*, 1988, **6**, 635–642.
16. Blanc, M. and Richmond A. D., *J. Geophys. Res.*, 1980, **85**, 1669–1686.
17. Onwumechille, A., Kauasaki, K. and Akasofu, S. I., *Planet. Space Sci.*, **21**, 1–16.
18. Onwumechille, A. and Ogubuctti, P. O., *J. Atmos. Terr. Phys.*, 1962, **24**, 173–190.
19. Akasofu, S. I. and Meng, C. I., *J. Atmos. Terr. Phys.*, 1968, **30**, 227–241.
20. Matsushita, S., *J. Geomag. Geoelectr.*, 1979, **31**, 225–235.
21. Nishida, A., *J. Geophys. Res.*, 1968, **73**, 1795–1803.
22. Nishida, A., Iwasaki, N. and Nagata, T., *Ann. Geophys.*, 1966, **22**, 478 484.
23. Reddy, C. A., Somayajulu, V. V. and Devasia, C. V., *J. Atmos. Terr. Phys.*, 1981, **41**, 189–201.
24. Gonzales, C. A., Kelley, M. C., Behnke, R. A., Vickery, J. F., Ward, R. and Holt, J., *J. Geophys. Res.*, 1983, **88**, 9135–9144.
25. Gonzales, C. A., Kelley, M. C., Fejer, B. G., Vickery, J. F. and Woodman, R. F., *J. Geophys. Res.*, 1979, **84**, 5803–5812.
26. Fejer, B. G., Farely, D. T., Woodman, R. F. and Calderon, C., *J. Geophys. Res.*, 1979, **84**, 5792–5796.
27. Fejer, B. G., Larzen, M. F. and Farely, D. T., *Geophys. Res. Lett.*, 1983, **10**, 537–540.
28. Fejer, B. G., Spiro, R. W., Wolf, R. A. and Fester, J. C., *Ann. Geophys.*, 1990, **8**, 441–454.
29. Kan, J. R. and Akasofu, S. I., *IEEE Trans. Plasma Sci.*, 1989, **17**, 83–108.
30. Nopper, R. W. and Carovillane, R. L., *Geophys. Res. Lett.*, 1978, **5**, 699–702.
31. Matsushita, S. and Kamide, Y., *J. Atmos. Terr. Phys.*, 1981, **43**, 403–410.
32. Spiro, R. W., Harel, M., Wolf, R. A. and Reiff, P. H., *J. Geophys. Res.*, 1981, **86**, 2261–2272.
33. Spiro, R. W., Wolf, R. A. and Fejer, B. G., *Ann. Geophys.*, 1988, **6**, 39–50.
34. Blanc, M., *J. Geophys. Res.*, 1983, **88**, 235–242.
35. Senior, C. and Blanc, M., *J. Geophys. Res.*, 1984, **89**, 261–284.
36. Tsunomuro, S. and Araki, T., *Planet. Space Sci.*, 1984, **32**, 599–604.
37. Nishbet, J. S., Miller, M. J. and Carpenter, L. A., *J. Geophys. Res.*, 1978, **83**, 2647–2657.
38. Denisenko, V. V. and Zamay, S. S., *Geomag. Aeron.*, 1987, **27**, 739–752.
39. Denisenko, V. V. and Zamay, S. S., *Planet. Space Sci.*, 1992, **40**, 941–952.
40. YE.Sakharou, Y., Nikiten, M. A. and Simirnov, D. A., *Geomag. Aeron.*, 1989, **29**, 344–349.
41. Zamay, S. S., *Geomag. Aeron.*, 1989, **29**, 104–108.
42. Rastogi, R. G. and Patel, V. L., *Proc. Indian Acad. Sci.*, 1975, **74**, 62–75.
43. Patel, V. L., *J. Geophys. Res.*, 1978, **83**, 2137–2142.
44. Matsushita, S., *J. Atmos. Terr. Phys.*, 1977, **39**, 1207–1215.
45. Kelley, M. C., Fejer, B. G. and Gonzales, C. A., *Geophys. Res. Lett.*, 1979, **6**, 301–304.
46. Galperin, Yu. I., Ponomarev, V. N. and Zosimova, A. G., *J. Geophys. Res.*, 1978, **83**, 4265–4272.
47. Somayajulu, V. V., Krishna Murthy, B. V. and Subbarao, K. S. V., *J. Atmos. Terr. Phys.*, 1991, **53**, 965–976.
48. Nishida, A., *Cosmic Electrodynamics*, 1971, **2**, 350–358.
49. Mcpherron and Manka, R. H., *J. Geophys. Res.*, 1985, **90**, 1175–1190.
50. Clauer, C. R. and Kamide, Y., *J. Geophys. Res.*, 1985, **90**, 1343–1354.
51. Meng, C. I., *J. Geophys. Res.*, 1983, **88**, 137–149.

Received 21 December 1992; accepted 6 January 1992